Organic & Biomolecular Chemistry

Accepted Manuscript

This article can be cited before page numbers have been issued, to do this please use: P. Rana, L. Panda, N. Murmu, B. P. Bag and S. N. Sahu, *Org. Biomol. Chem.*, 2020, DOI: 10.1039/D0OB00608D.

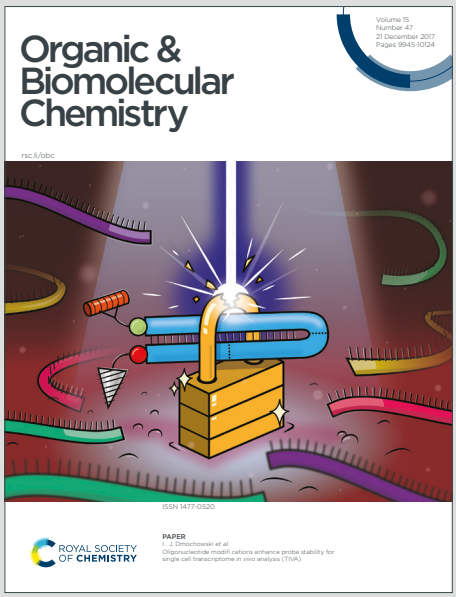

ROYAL SOCIETY OF CHEMISTRY

rsc.li/obc

View Article Online
DOI: 10.1039/D0OB00608D

Fluorometric sensing of hydroxyl amine in aqueous medium utilizing a diphenyl imidazole-based probe

Punam Rana,[a] Lipsarani Panda, [a] Narayan Murmu,[a] Bhawani Prasad Bag[b] and Satya Narayan Sahu*[a]

[a] *School of Chemistry, Sambalpur University, Jyoti Vihar, Burla-768 019, Odisha, India*

Email: snsahu.chem@gmail.com; snsahu@suniv.ac.in

[b] *Department of Biotechnology and Bioinformatics, Sambalpur University, Jyoti Vihar, Burla-768 019, Odisha, India*

Graphical Abstract

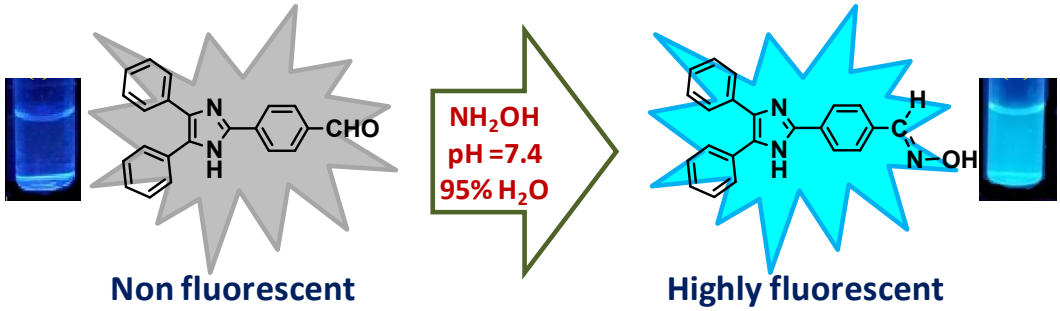

Abstract

The detection of hydroxyl amine in aqueous medium is challenging due to its very similar chemical reactivity with nearer competitors such as hydrazine hydrate and primary amines. Moreover, the detection of hydroxyl amine at neutral pH adds further complexity to the sensing phenomenon due to its poor reactivity in neutral aqueous medium. In this work, we have presented a diphenyl imidazole benzaldehyde (**DIB**) probe which demonstrates the detection of hydroxylamine (HA) in micromolar concentration with high selectivity in 5% DMSO phosphate buffer solution at pH 7.4 *via* a fluorescence "turn-on" signal. The interaction of hydroxyl amine with the probe has been comprehensively studied by using fluorescence technique, proton NMR, FTIR, ESI-Mass and DLS measurements. The experimental results were further corroborated with the DFT studies. These results could pave the way toward the development of molecular indicators for hydroxyl amine in chemical and biological platforms.

1. Introduction

Hydroxylamine (HA), NH_2OH, is an oxidised form of ammonia which is abundantly used by various industries for processing of dyes, textile, plastics, semiconductors and photography.[1,2] Further, it is one of the important chemical constituent for the synthesis of caprolactam, a

View Article Online
DOI: 10.1039/D0OB00608D

monomer for the production of Nylon-6 based products.[3] Very recently, it is used as a primary material for making of hydroxylamine nitrate (HAN) which is considered as the next generation nontoxic propellant as an alternative to toxic hydrazine based propellants to be employed in spacecraft, nuclear power and military services.[4] Besides, it serves as an active ingredient for the synthesis of hydroxamic acid/hydroxamate based drug substances.[5] Moreover, HA can act as nitric oxide (NO) donor molecule and involve in many biological functions.[6,7] Despite its widespread applications, unfortunately HA is a potentially hazardous material which can elicit highly specific mutations with cytosine[8] and thus can cause modest level of toxicity to humans, animals and plants. 2 μg/day is the maximum recommended exposure limit for hydroxylamine.[9] Consequently, many research groups have taken an utmost interest to develop a selective and sensitive analytical procedure for the trace level estimation of hydroxylamine in aqueous medium. Although a diverse range of conventional techniques such as high-performance liquid chromatography, gas chromatography, potentiometric, polarographic, biamperometric and electrochemical methods have been developed,[10-17] but these practices do not offer an economical and practical monitoring of HA at the desired location. In this context, fluorescence technique could provide a rather precise substitute owing to its several benefits such as fast, sensitive, selective and operational simplicity for detection and quantification of hydroxylamine. In addition, the detection of hydroxyl amine is quite challenging due to very similar chemical reactivity with its close competitors such as hydrazine hydrate and primary amines.[18-20] Although many reports have been published on the detection of hydrazine,[21,22] however, to our best only two reports have been published by Sedgwick *et. al.* and Dong *et. al.* for selective fluorogenic detection of hydroxyl amine.[23,24] Therefore, development of molecular fluorophores for specific and sensitive detection of HA in micromolar concentrations has received a great deal of interest. With this vision and in continuation to our efforts toward the development of chromofluoroscent molecular sensors,[25-27] we have prepared a probe 4-(4,5-diphenyl-1*H*-imidazol-2-yl)benzaldehyde (**DIB**) which demonstrates the detection of hydroxylamine (HA) in micromolar concentration with high selectivity in 5% DMSO phosphate buffer solution at pH 7.4 *via* a fluorescence "turn-on" behavior. The probe elicits a visual colour change from colourless to cyan fluorescence to the sensor solution in presence of HA. Further, the probe shows a prominent fluorescence "turn-on" signal with HA in comparison to its closer competitor hydrazine.

View Article Online
DOI: 10.1039/D0OB00608D

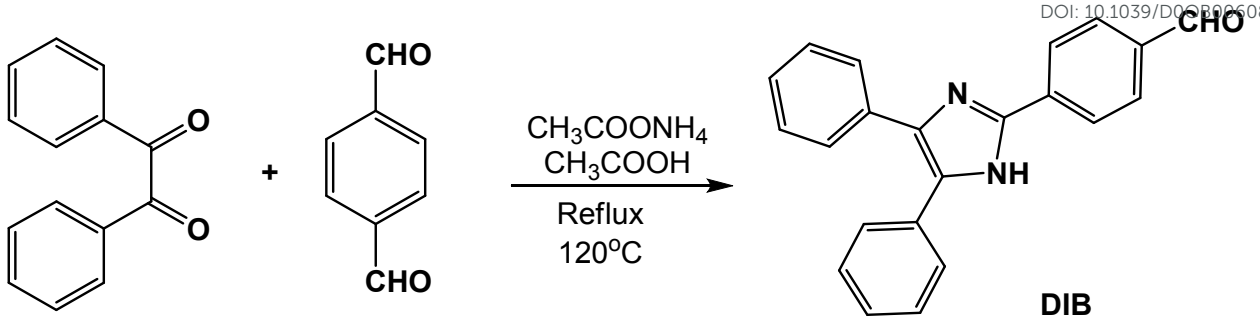

Scheme 1. Synthesis protocol for probe **DIB**

2. Results and Discussion

2.1. Synthesis and characterization of probe DIB

The general experimental methods, preparation of test samples and synthetic procedure of probe 4-(4,5-diphenyl-1*H*-imidazol-2-yl)benzaldehyde **(DIB)** (Scheme 1) has been described in Supporting Information (see ESI). Condensation reaction of benzil with terephthaldehyde in glacial acetic acid medium affords **DIB** in moderate yield. The analytical characterization of **DIB** was consistent with its indicated structure (Fig. S1-S4). The proton NMR spectrum (Fig. S1) of **DIB** showed a singlet at 13.03 ppm which could be assigned to imidazolyl-NH proton that was exchanged upon addition of D_2O. The singlet at 10.03 ppm could be attributed to aldehydic –CHO proton. The doublets at 8.30 and 8.01 ppm and multiplets at 7.58-7.23 ppm conform to the aromatic protons. The ^{13}C NMR shows the characteristic signal at 193 ppm for the carbonyl carbon of the aldehyde group (Fig. S2). The FTIR spectra (Fig. S3) shows bands at 3355, 1695 and 1442 cm^{-1} which respectively corresponds to the secondary amine –NH, >C=O and Ar-C=C- stretching frequencies. The ESI-MS mass data (Fig. S4) further confirmed the formation of probe **DIB** by the appearance of a signal at *m/z* 325.33 for the $[M+H]^+$ ion.

2.2. Photophysical studies of DIB

The probe **DIB** comprises an imidazole ring conjugated with a benzaldehyde unit. Thus it is expected that the imidazole unit and the aldehyde group behave as a donor and acceptor combination respectively which could show significant photophysical properties. We first studied the solvatofluorism of the probe in eight different organic medium such as benzene, toluene, tetrahydrofuran, 1,4-dioxane, acetone, methanol, acetonitrile and dimethylsulphoxide (DMSO) of varying polarity at 50 μM concentration at room temperature. The solutions of **DIB** in organic solvents exhibited a strong photoluminescence under UV light at 365 nm (Fig. S5). The fluorescence spectra of the probe exhibited a gradual bathochromic shift in its emission band by increasing the solvent polarity (Fig. 1a). In non-polar toluene, the probe exhibited an emission

View Article Online
DOI: 10.1039/D0OB00608D

band at 425 nm while in polar methanol medium it appeared at 575 nm with a significant bathochromic shift ($\Delta\lambda_{em}$) of 150 nm. This solvent depended fluorescence behaviour clearly suggests that the photoexcited states of **DIB** are polar in nature which gets stabilized by solvation resulting in light emission at a higher wavelength from the stabilized molecules.[28,29]

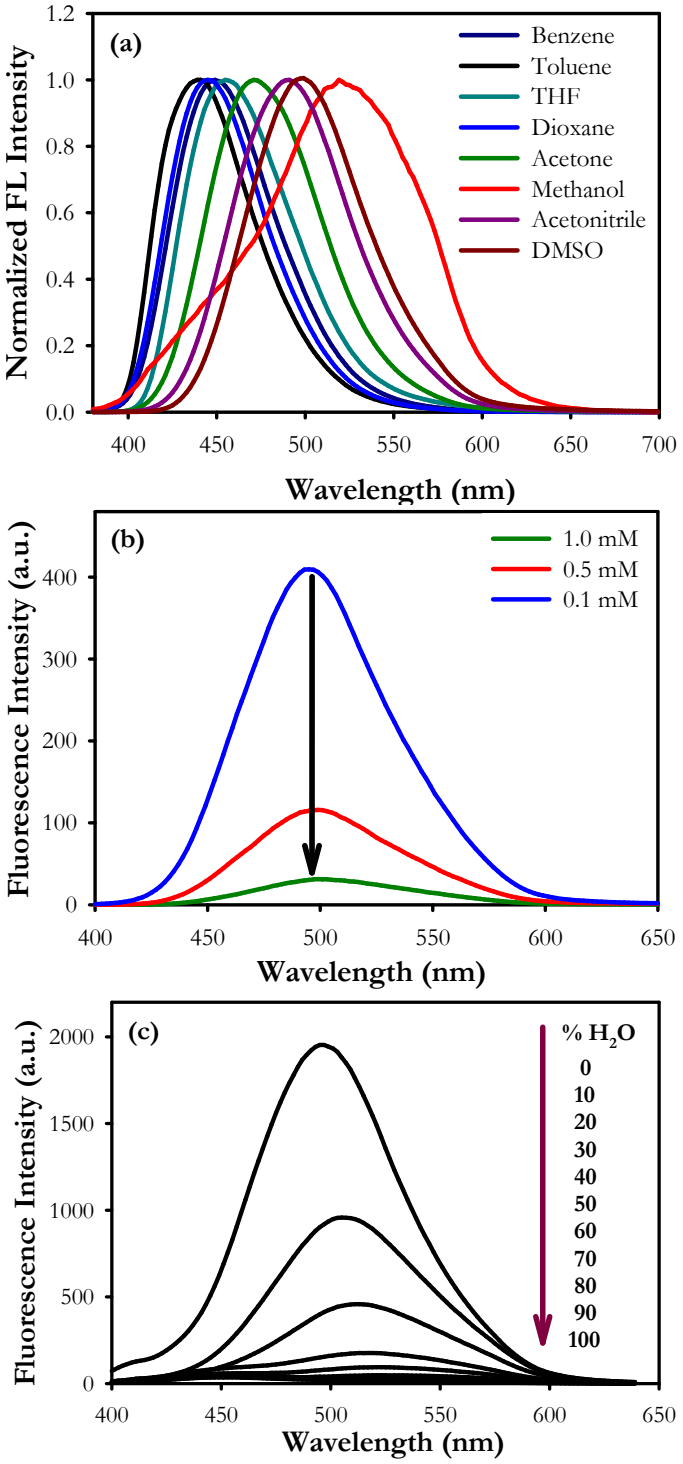

Fig. 1. (a) Normalized emission spectra of **DIB** (50 µM) in benzene, toluene, THF, dioxane, acetone, methanol, acetonitrile and DMSO. (b) Fluorescence spectra of **DIB** at various concentrations in DMSO. (c) Fluorescence spectra of **DIB** (50 µM) at various DMSO-Water fractions (λ_{ex} = 365)

View Article Online
DOI: 10.1039/D0OB00608D

The shifts in emission bands could be assigned to the π-electron delocalization from the imidazole donor to aldehyde acceptor *via* a "push−pull" mechanism within the **DIB** molecule as a result of increasing solvent polarity. Further, aggregation induced emission (AIE) and aggregation caused quenching (ACQ) characteristics of **DIB** have been evaluated by fluorescence studies. For the ACQ study, fluorescence spectra were measured at various concentrations of **DIB** ranging from 1.0 mM to 0.1 mM. It was observed that, with increase in probe concentration the fluorescence intensity decreases which indicates that the concentrated probe solution is poorly emissive in nature (Fig. 1b). In contrast, the AIE behavior of **DIB** was examined by recording the emission spectra at varying DMSO-water fractions (f_w = 0 to 100%) at 50 μM probe concentration. It was observed that the cyan colour fluorescence signal goes on decreasing with increase in water fraction (f_w) when analysed under an UV lamp at 365 nm (Fig. S6). The fluorescence spectra of the corresponding solutions showed a regular decrease in the fluorescence intensity at 490 nm with increase in water fraction (f_w) from 0 to 100% (Fig. 1c). This result clearly suggested the absence of AIE behavior in the probe.[30]

2.3. Fluorescence analysis of DIB in presence of various amines

The interaction of **DIB (**50 μM**)** with various amines such as urea, thiourea, aniline, triethylamine (TEA), ammonium hydroxide, hydroxyl amine, ethylene diamine, piperidine, hydrazine hydrate and methyl amine dissolved in Millipore water, was analysed in 5% DMSO phosphate buffer solution at pH 7.4. By addition of 20 equiv. of different amines to the probe solution, intense cyan colour fluorescence was appeared only in presence of hydroxyl amine (HA) (Fig. 2a). On the other hand, addition of hydrazine hydrate (HH) resulted in a faint blue fluorescence coloration while other amines showed insignificant fluorescence colour change in the probe solution when observed under UV-light at 365 nm (Fig. 2a). The fluorescence spectra of the corresponding solutions showed more than 30-fold enhancement in emission intensity at 465 nm in presence of HA while HH enhances the intensity to 8-fold only (Fig. 2c). In contrast, other amines did not exhibit any significant enhancement in fluorescence intensity (Fig. 2b,c). These results clearly indicate a greater selectivity of **DIB** toward HA in comparison to its closer competitor hydrazine hydrate (HH) *via* a change in fluorescence signal. Further, the fluorogenic selectivity of **DIB** against various anions and cations were investigated by visual observation under an UV-light at 365 nm. Upon addition of 20.0 equiv. of different anions and cations such as F^-, Cl^-, Br^-, I^-, $H_2PO_4^-$, HSO_4^-, OH^-, AcO^-, CN^-, S^{2-}, Ag^+, Ba^{2+}, Ca^{2+}, Cd^{2+}, Co^{2+}, Cu^{2+},

View Article Online
DOI: 10.1039/D0OB00608D

Cr^{2+}, Fe^{2+}, Hg^{2+}, Mg^{2+}, Mn^{2+}, Ni^{2+}, Pb^{2+}, Pd^{2+} and Zn^{2+}, no significant fluorescence colour change was detected in the probe solution (Fig. S7).

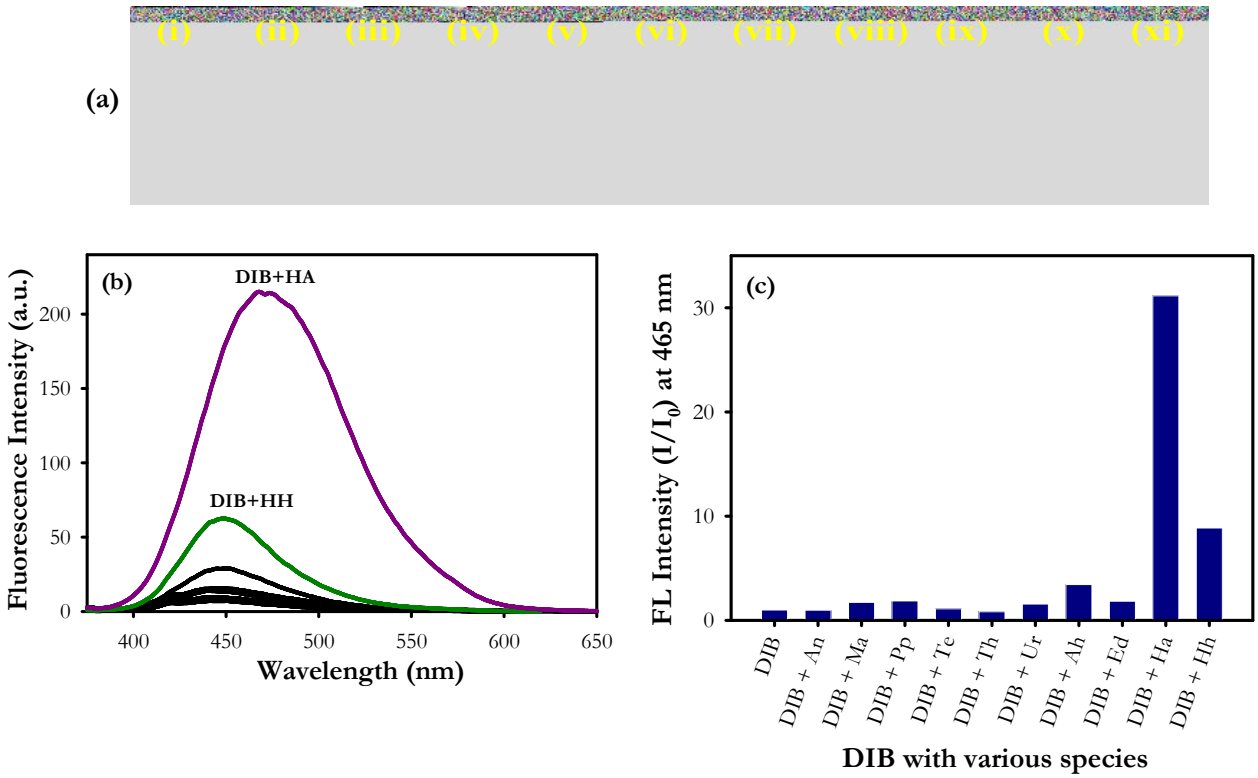

Fig. 2. (a) Visual fluorescence change of **DIB (**50 μM**)** in 5% DMSO phosphate buffer solution at pH 7.4 with various amines (20 equiv.) under UV-light at 365 nm. (i) Probe **DIB** alone and probe with other species (ii) aniline (An) (iii) methyl amine (Ma) (iv) piperidine (Pp) (v) hydroxyl amine (Ha) (vi) triethyl amine (Te) (vii) hydrazine hydrate (Hh) (viii) thiourea (Th) (ix) urea (Ur) (x) ethylene diamine (Ed) (xi) ammonium hydroxide (Ah). (b) Fluorescence spectra of **DIB (**50 μM**)** in 5% DMSO phosphate buffer solution at pH 7.4 in presence of 20 equiv. of various amines. (c) Emission intensities (I/I_0) at 465 nm of corresponding spectra in presence of various species. (λ_{ex}= 365 nm).

2.4. Effect of pH on the fluorescence properties of DIB in presence of hydroxyl amine

It is well known that the interaction of aldehyde group with hydroxyl amine is highly pH depended.[31] Thus, to analyze the effect of pH on the fluorescence properties of **DIB** (50 μM) in presence of HA (20 equiv.), the fluorescence spectra were recorded over a pH range of 1 to 13. It was observed that, probe **DIB** showed no significant change in its emission intensity at 465 nm over the pH range of 1 to 13 which indicates its good stability over the tested pH (Fig. S8). However, addition of HA enhances the fluorescence intensity of the probe at 465 nm and exhibited a stable response over a pH range of 4-9 (Fig. S8). At pH 2 and 3, the emission signal of the probe at 465 nm is quite high in presence of HA which could be due the favorable reaction condition between the aldehyde and NH_2 group at acidic conditions.[31] In contrast, fluorescence intensity of the probe at 465 nm decreases beyond pH 9. These findings suggested that the probe

View Article Online
DOI: 10.1039/D0OB00608D

can detect HA over a wide range of pH of 4 to 9. Although the probe showed a significant fluorescence response toward HA at pH 2-3, we have not taken this pH range to study the recognition experiments due to highly acidic condition. Rather, the physiological pH medium at 7.4 was considered throughout all the recognition experiments. Moreover, a 5% DMSO phosphate buffer solution at pH 7.4 was used for all the studies.

2.5. Optical response time of DIB with hydroxyl amine and hydrazine hydrate

In order to establish the optical response time, the time-dependent single wavelength fluorescence measurement was performed for **DIB** in presence of HA and HH at 465 and 458 nm respectively. The emission intensity of **DIB** with hydroxyl amine (at 465 nm) and hydrazine hydrate (at 458 nm) increases with time and finally reached a plateau beyond 2 hour (Fig. S9). However, the emission enhancement in presence of HA was found to be much higher than with HH even at the earlier period of time. By analyzing the fluorescence intensities at the initial 30 minutes period, it was observed that the intensity for HA is much higher and fast responsive in comparison to HH (Fig. S9). This observation clearly demonstrates that probe **DIB** shows a faster response and higher sensitivity toward HA in comparison to its closer competitor HH.

2.6. Fluorescence titration study of DIB with hydroxyl amine and hydrazine hydrate

From the fluorescence time response study (Fig. S9), a better sensitivity was established for HA in comparison to HH by the probe **DIB**. Thus, to get insight into the sensing mechanism, fluorescence titration spectra were recorded by the addition of different equivalents of HA and HH to **DIB** (50 μM) in 5% DMSO phosphate buffer solution at pH 7.4 with incubation time of 2 hour. Addition of HA to **DIB** increases the fluorescence intensity at 465 nm concomitantly with various equivalents up to more than 30-fold enhancement (inset Fig. 3a). Further, UV-illumination at 365 nm to different vials containing **DIB** (50 μM) with various equivalents of HA shows a gradual increase in cyan colour fluorescence with increasing equivalents of HA that can be easily distinguish by visual observation (Fig. S10). On the other hand, a similar set of titration experiment of **DIB** with HH showed the increase in fluorescence intensity at 458 nm with continual addition HH exhibiting an enhancement of 8-fold only even after the addition of 20 equivalents (Fig. 3b). The fluorescence enhancement of **DIB** in presence of HA is significantly higher in comparison to HH which indicates a higher recognition affinity of the probe toward hydroxyl amine. Moreover, the concentration-dependent fluorescence response for both HA and HH shows a linear relationship up to 20 equivalents (Inset of Fig. 3a,b). The binding constant

View Article Online
DOI: 10.1039/D0OB00608D

(K_a) of probe **DIB** toward HA and HH were calculated from their fluorescence titration profile at 465 and 458 nm respectively by using the linear regression analysis. The binding constant (K_a) for HA and HH were found out to be 2.23 x 10^4 M^{-1} and 3.12 x 10^3 M^{-1} with regression coefficient of 0.98 and 0.99 respectively (inset Fig. 3a,b). The higher binding constant of **DIB** for HA in comparison to HH clearly signifies a high level of sensitivity of the probe toward HA. Finally, the detection limit of **DIB** (50 μM) for HA was determined by fluorescence measurement at 465 nm in 5% DMSO phosphate buffer solution at pH 7.4 and was found out to be 28 μM (~0.92 ppm) (Fig. S11).

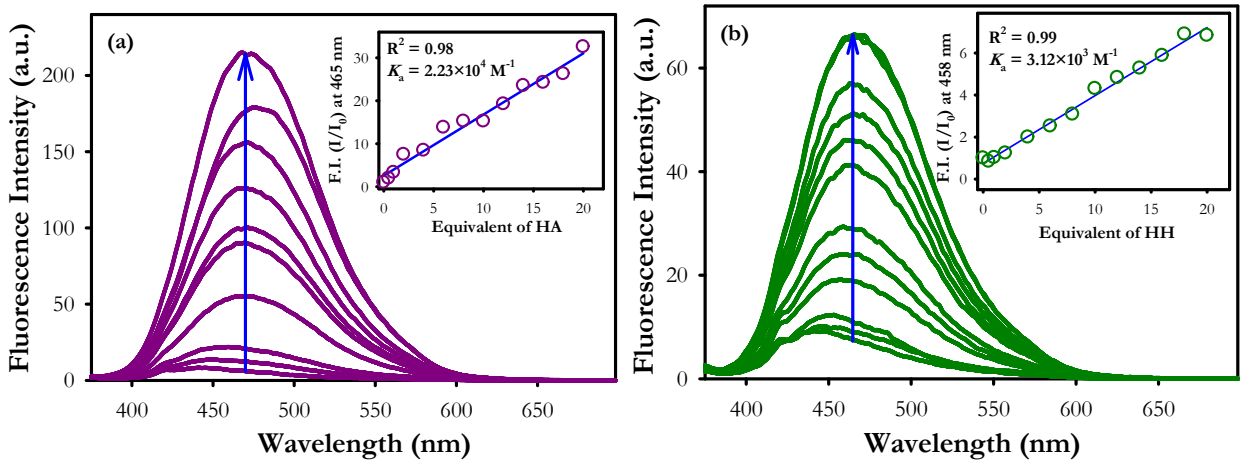

Fig. 3. (a) Fluorescence titration spectra of **DIB** (50 μM) in 5% DMSO phosphate buffer solution at pH 7.4 with of 0.0 to 20.0 equivalents of HA. Inset shows the fluorescence intensity at 465 nm *vs.* equiv. of HA. (b) Fluorescence titration spectra of **DIB** (50 μM) in 5% DMSO phosphate buffer solution at pH 7.4 with of 0.0 to 20.0 equivalents of HH. Inset shows the fluorescence intensity at 458 nm *vs.* equiv. of HH.

2.7. Binding mode and sensing mechanism of DIB

Based on the photophysical observations of **DIB** with HA and HH, we have proposed the mode of interaction of the probe with the analytes as shown in Scheme 2. The formation of products **C** and **D** (Scheme 2) was analyzed by ^{1}H NMR experiment after separating the products from the reaction of HH and HA, respectively with the probe **DIB** (Fig. 4). The NMR studies show that the aldehydic proton (-CHO) signal at 10.03 ppm in **DIB** got disappeared and a new signal at 8.25 ppm is appeared for the azomethine proton (-CH=N-), which evidently indicates the formation of condensation products **C** and **D**. Further, the imidazole-NH signal and aromatic proton signals of the phenyl ring bearing aldehyde group show upfield shifts in products **C** and **D** which signifies a decrease in electron delocalization in the products (**C** and **D**) in comparison to probe **DIB**.

View Article Online
DOI: 10.1039/D0OB00608D

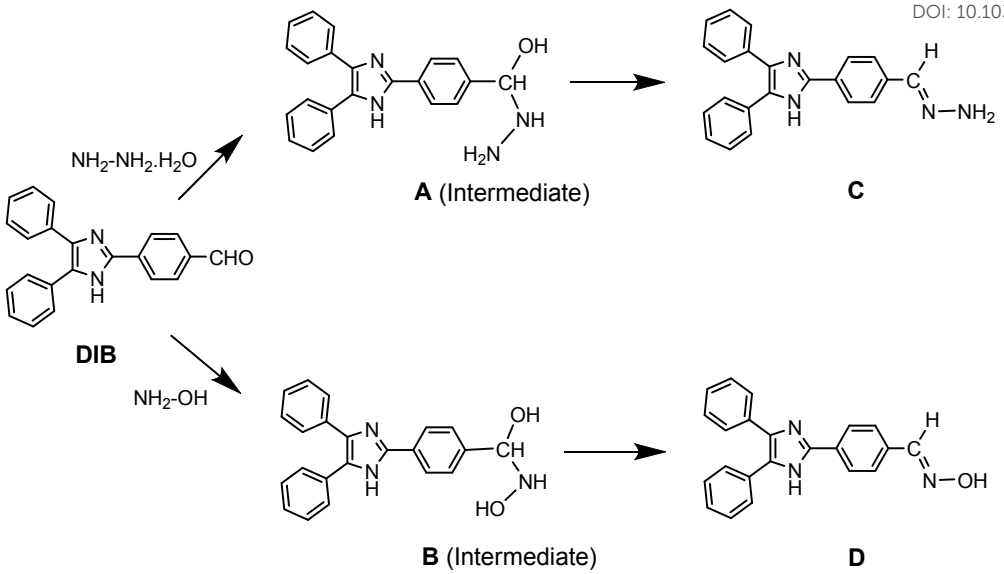

Scheme 2. A plausible reaction and sensing mechanism of probe **DIB** with hydroxyl amine (HA) and hydrazine hydrate (HH)

This decrease in electron delocalization could be due to the chemical transformation from aldehyde group in **DIB** to hydrazone and oxime units in **C** and **D** respectively, where the carbonyl group possesses more electron withdrawing ability than the oxime and hydrazone units. The FTIR spectroscopy also confirmed the formation of the condensation product **D** (Scheme 2) resulting from the interaction of **DIB** with HA (Fig. S12). The band at 1695 cm^{-1} assigned to >C=O stretching frequency of the aldehyde group in **DIB** get disappeared in product **D** (**DIB**+HA). Besides, the appearance of a broad band near 3460 cm^{-1} and a sharp band at 1641 cm^{-1}, respectively assigned to –OH and >C=N- stretching frequencies, clearly indicates the formation of an oxime product **D**. The formation of products **C** and **D** was also confirmed from the ESI-Mass experiments which showed a peak at *m/z* 338.93 and 339.93, respectively for the hydrazone and oxime molecular ions (Fig. S13).

The fluorescence enhancement of **DIB** with HH and HA is probably because of the formation of the condensation products **C** and **D** *via* the formation of the intermediate products **A** and **B**, respectively. The electron withdrawing power of hydrazone and oxime units is comparatively poorer in comparison to an aldehyde group. Thus, the overall electron delocalization from the donor imidazole unit to the acceptor oxime group in product **D** is relatively less prominent than that observed in probe **DIB** between the donor imidazole unit and acceptor aldehyde group as confirmed from the NMR studies. The computational calculation also shows a stronger electron delocalization in probe **DIB** than the products **C** and **D** (discussed in detail in section 2.8).

View Article Online
DOI: 10.1039/D0OB00608D

Thus, when the probe (**DIB**) molecule is excited, it is expected to exhibit a stronger intramolecular charge transfer (ICT) process in the excited state in comparison to the product **D** that can lead to more non-radiative relaxation processes resulting in significant quenching of the fluorescence signal.[32] Further, the relatively poor solubility of the probe (**DIB**) in aqueous solution in tandem with ICT process at the excited state might be responsible for its overall decrease in the fluorescence signal. On the other hand, the introduction of –OH group in oxime product **D** might enhances its solubility in aqueous medium together with a decrease in ICT process at the excited state (due to poor electron withdrawing power of oxime group) could possibly lead to the fluorescence enhancement of the probe (**DIB**) solution upon interaction with HA.[32]

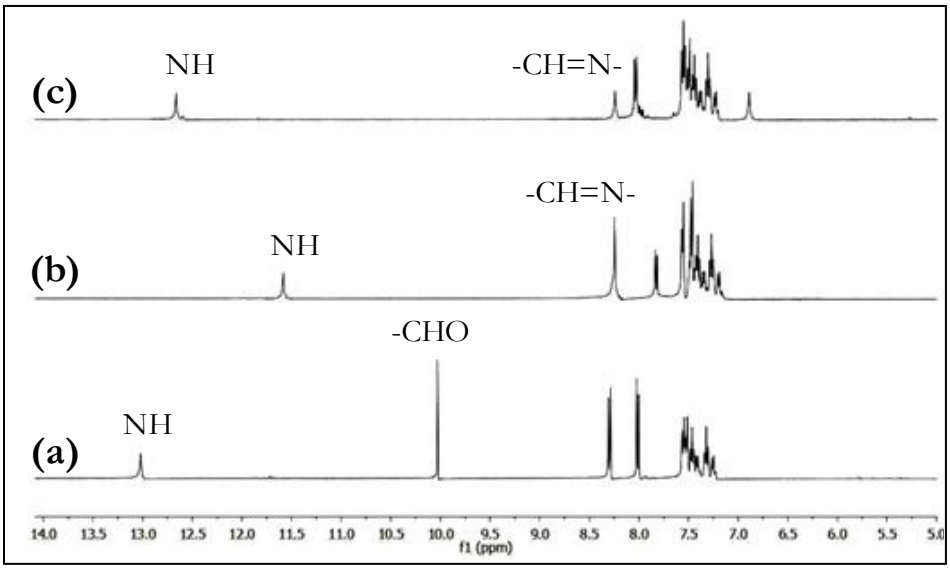

Fig. 4. ^{1}H NMR spectra of (a) probe **DIB**, (b) product **D** (**DIB**+HA) and (c) product **C** (**DIB**+HH) in DMSO-d_6.

Moreover, the reason behind the fluorescence enhancement of **DIB** in presence of HH was analyzed by dynamic light scattering (DLS) experiments to confirm whether the fluorescence is due to the product **C** or as a consequence of molecular aggregation. It was observed that the average particle size of **DIB** probe (50 μM) at 95% water is 182 nm and that of **DIB**+HH (50 μM each) is 199 nm, even after an incubation period of 5 hrs (Fig. S14). This result clearly indicated that both **DIB** and its condensation product **C** (**DIB** + HH) have very similar hydrodynamic radius (particle size). Thus, the enhancement in fluorescence properties of the probe is possibly due to the formation of condensation product **C,** rather than any AIE effect. All

View Article Online
DOI: 10.1039/D0OB00608D

these experimental findings clearly indicate that the formation of condensation products **C** and **D** with HH and HA, respectively enhances the fluorescence signal of the probe **DIB**.

2.8. Computational studies

Now to understand the interaction of probe **DIB** with the analytes HA and HH, quantum chemical calculations were performed on theoretical models by employing time-dependent density functional theory (TD-DFT) using B3LYP functional and 6-31+G basis set in gas phase and water solvent phase using Gaussian 09 program.[33] The obtained optimized structures of probe **DIB**, the intermediates **A** & **B** and the final products **C** & **D** (Scheme 2) were visualized by using Gaussview 5 program and are shown in Fig. 5.

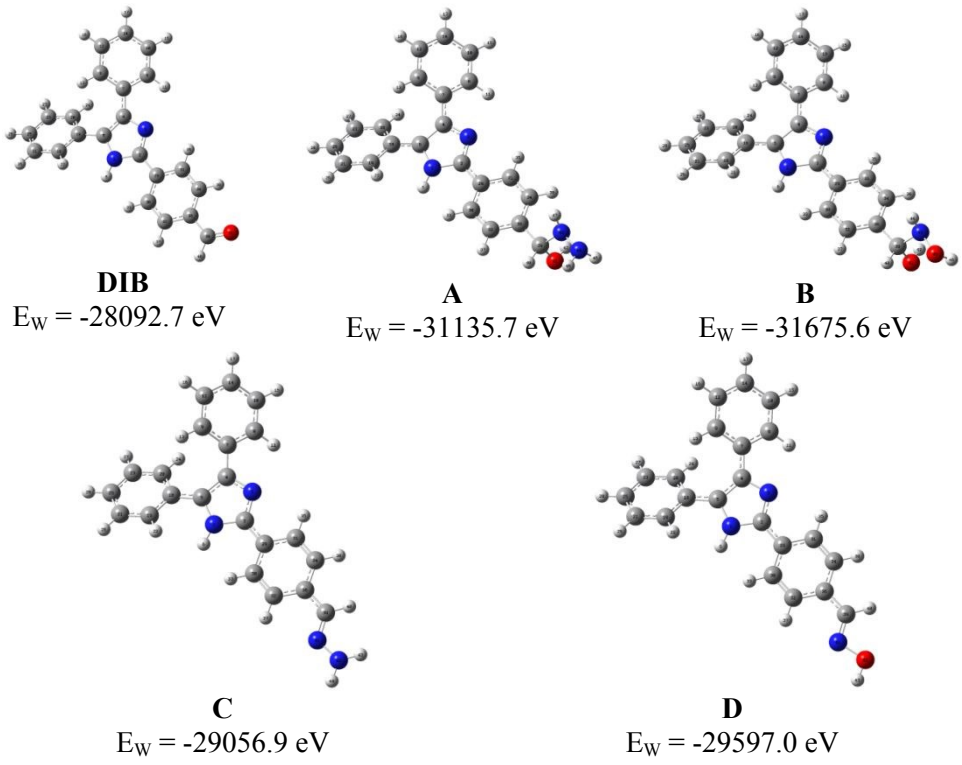

Fig. 5. Optimized structures of probe **DIB**, intermediates **A** & **B** and products **C** & **D** (colour key: white = hydrogen; grey = carbon; blue = nitrogen; red = oxygen). E_W indicates the calculated total energy in water medium.

More information about the mechanism of interaction of **DIB** with the analytes was obtained from the typical transition energy diagram for the highest occupied molecular orbital (HOMO) and the lowest unoccupied molecular orbital (LUMO) of the probe along with its resultant intermediates with hydroxyl amine and hydrazine as shown in Fig. 6. In probe **DIB**, the electron distribution in HOMO is located over the entire molecule with a larger density on the imidazole

View Article Online
DOI: 10.1039/D0OB00608D

and phenyl rings while in LUMO it is mainly concentrated over the benzaldehyde unit. On the other hand, the electron distribution in HOMO and LUMO orbitals are located over the entire molecule in intermediates **A** & **B**. Similarly, in the final products **C** & **D**, the electron density in HOMO is distributed over the entire molecule while in LUMO it is largely spread over the aromatic ring possessing the hydrazone (**C**) and oxime (**D**) groups (Fig. 6).

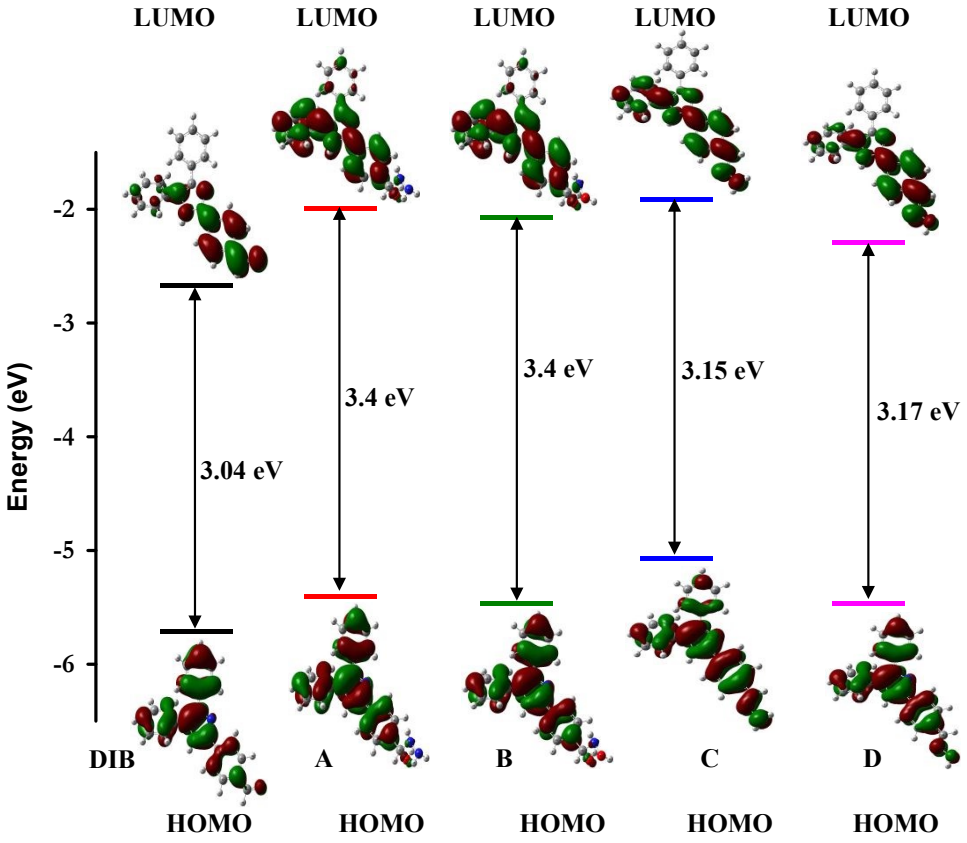

Fig. 6. The orbital shape and energy of the HOMO and LUMO of probe **DIB** and intermediates **A** & **B** and products **C** & **D** calculated with DFT(B3LYP)/6-31+G method.

With reference to the energy of free probe **DIB** (-28092.7 eV), the optimized energies of the intermediates **A** (-31135.7 eV), **B** (-31675.6 eV) and the products **C** (-29056.9 eV), **D** (-29597.0 eV) were found to be lower, which indicates the greater stability of the intermediates as well as the products (Fig. 5). Further, these results indicate that the reaction of HA with the probe is more favorable over HH as it forms a more stable intermediate **B** and product **D** in comparison to **A** and **C** from HH. This observation is in good agreement with the time-dependent single wavelength fluorescence studies which show the rapid formation of oxime over hydrazone with probe **DIB**. The calculated energy of the HOMO and LUMO levels of the intermediates (**A** & **B**) and products (**C** & **D**) were found to be increased from that of the free probe (Fig. 6) which can be attributed due to the change in the electron distribution over the entire molecule by changing

View Article Online
DOI: 10.1039/D0OB00608D

the nature of the functional group from aldehyde to hydrazone/oxime unit. Moreover, the HOMO of probe **DIB** (-5.71 eV) is more stabilized over the HOMO of products **C** (-5.07 eV) and **D** (-5.47 eV) that indicates a stronger electron delocalization in **DIB** in comparison to **C** and **D** which is also confirmed from the proton NMR experiments.

3. Conclusions

In summary, we have synthesized a diphenyl imidazole based probe **DIB** through simple condensation reactions in moderate yield. The probe **DIB** selectively detects hydroxyl amine (HA) and hydrazine hydrate (HH) amongst various amines through a distinct visual fluorescence change from non emissive to bright cyan and faint blue fluorescence respectively in 5% DMSO phosphate buffer solution at pH 7.4. Interestingly, single wavelength time scan revealed that, probe **DIB** could optically discriminate the presence of HA from HH through a more than 30 fold enhancement in fluorescence intensity and faster response toward HA. The proton NMR, FTIR, ESI-Mass, DLS and DFT studies indicate that the enhancement in fluorescence signal of the probe upon interaction with hydroxyl amine is due to the formation of oxime product which modulates the ICT process in the excited state. The detection limit of **DIB** toward HA is found to be 28 μM by fluorescence method indicating a greater sensitivity. Further the probe could detect the HA over a pH range of 4.0 to 9.0 *via* a diagnostic cyan colour visual fluorescence response. All together these results could pave the way toward the development of molecular indicators for hydroxyl amine in multiple platforms.

Conflicts of interest

There are no conflicts to declare.

Acknowledgements

S.N.S gratefully acknowledges the financial assistance received from S&T Department, Govt. of Odisha for the research grant. The research grant received from GNM Foundation for Prof. GN Mahapatra Endowment Chair award is gratefully acknowledged. P. R and L. P are thankful to School of Chemistry for providing necessary facilities to carry out this work. N. M is grateful to S&T Department, Govt. of Odisha for a project fellowship. B.P.B is grateful to Department of Biotechnology and Bioinformatics, Sambalpur University for providing necessary computational facilities. Authors are thankful to Materials Research Centre, MNIT Jaipur, NMR facility of Department of Chemistry, Ravenshaw University and ESI-Mass facility of NISER, Bhubaneswar for recording the NMR and Mass spectra. A special thanks to Prof. Parameswar Krishnan Iyer and Mr. Niranjan Meher of I.I.T Guwahati for carrying out DLS experiments, Dr. P. Parhi,

View Article Online
DOI: 10.1039/D0OB00608D

Ravenshaw University, for carrying out NMR studies and Dr. C. S. Purohit, NISER, Bhubaneswar, for carrying out ESI-Mass studies reported in this paper. The financial assistance received from UGC and DST, New Delhi under the DRS and FIST grant respectively to School of Chemistry is gratefully acknowledged. We are thankful to Dr. H. Chakraborty, Sambalpur University for his useful suggestions toward the improvement of this manuscript.

References

1 R. M. Liu, M. R. McDonald and D. W. Margerum, *Inorg. Chem.,* 1995, **34**, 6093-6099.

2 K. A. Reinhardt and R. F. Reidy, *Handbook of Cleaning for Semiconductor Manufacturing: Fundamentals and Applications*, Wiley, 2010, page-344-347.

3 J. Ritz, H. Fuchs, H. Kieczka and W. C. Moran. *Ullmann's Encyclopedia of Industrial Chemistry*, Weinheim: Wiley-VCH, 2012, doi:10.1002/14356007.a05_031.pub2.

4 R. Amrousse, T. Katsumi, N. Azuma and K. Hori, *Combust. Flame,* 2017, **176**, 334-348.

5 S. Bertrand, J. J. Hélesbeux, G. Larcher and O. Duval, *Mini Rev. Med. Chem.*, 2013, **13**, 1311-1326.

6 P. G. Wang, M. Xian, X. P. Tang, X. J. Wu, Z. Wen, T. W. Cai and A. J. Janczuk, *Chem. Rev.*, 2002, **102**, 1091–1134.

7 Y. Ashani and I. Silman, *Hydroxylamines and Oximes: Biological Properties and Potential Uses as Therapeutic Agents*, Wiley, 2010, DOI: 10.1002/9780470682531.pat0465.

8 P. Gross, *Crit. Rev. Toxicol*., 1985, **14**, 87–99.

9 *M7 (R1) Addentum to ICH M7: Assessment and Control of DNA reactive (Mutagenic) impurities in pharmaceuticals to Limit Potential Carcinogenic Risk, International Consortium of Harmonisation (ICH)*, May 2015.

10 W. D. Korte, *J. Chromatogr.*, 1992, **603**, 145–150.

11 A. Afkhami, T. Madrakian and A. Maleki, *Anal. Sci.*, 2006, **22**, 329–331.

12 Y. Seike, R. Fukumori, Y. Senga, H. Oka, K. Fujinaga and M. Okumura, *Anal. Sci.*, 2004, **20**, 139–142.

13 R. Christova, M. Ivanova and M. Novkirishka, *Anal. Chim. Acta*, 1976, **85**, 301–307.

14 D. R. Canterford, *Anal. Chim. Acta*, 1978, **98**, 205–214.

15 C. Zhao and J. F. Song, *Anal. Chim. Acta*, 2001, **434**, 261–267.

16 Y. Wang, L. Wang, H. H. Chen, X. Y. Hu and S. Q. Ma, *ACS Appl. Mater. Interfaces*, 2016, **8**, 18173–18181.

17 C. H. Zhang, G. F. Wang, M. Liu, Y. H. Feng, Z. D. Zhang and B. Fang, *Electrochim. Acta*, 2010, **55**, 2835–2840.

18 T. A. Nigst, A. Antipova and H. Mayr, *J. Org. Chem.*, 2012, **77**, 8142-8155.

View Article Online
DOI: 10.1039/D0OB00608D

19 D. K. Kölmel and E. T. Kool, *Chem. Rev.*, 2017, **117**, 10358-10376.

20 D. Larsen, A. M. Kietrys, S. A. Clark, H. S. Park, A. Ekebergh and E. T. Kool, *Chem. Sci.*, 2018, **9**, 5252-5259.

21 S. K. Manna, A. Gangopadhyay, K. Maiti, S. Mondal and A. K. Mahapatra, *Chemistry Select*, 2019, **4**, 7219-7245.

22 B. Roy and S. Bandyopadhyay, *Anal. Methods*, 2018, **10**, 1117-1139.

23 A. C. Sedgwick, R. S. L. Chapman, J. E. Gardiner, L. R. Peacock, G. Kim, J. Yoon, S. D. Bull and T. D. James, *Chem. Commun.*, 2017, **53**, 10441-10443.

24 B. Dong, M. Tian, X. Kong, W. Song, Y. Lu and W. Lin, *Anal. Chem.*, 2019, **91**, 11397-11402.

25 S. K. Padhan, P. Rana, N. Murmu, B. S. Swain and S. N. Sahu, *Indian J. Chem., Sect. B: Org. Chem. Incl. Med. Chem.*, 2019, **58**, 167–182.

26 S. K. Padhan, J. Palei, P. Rana, N. Murmu and S. N. Sahu, *Spectrochim. Acta, Part A*, 2019, **208**, 271–284.

27 S. K. Padhan, N. Murmu, S. Mahapatra, M. K. Dalai and S. N. Sahu, *Mater. Chem. Front.*, 2019, **3**, 2437-2447.

28 C. Reichardt, *Chem. Rev.*, 1994, **94**, 2319-2358.

29 A. Marini, A. Muñoz-Losa, A. Biancardi and B. Mennucci, *J. Phys. Chem. B*, 2010, **114**, 17128-17135.

30 J. Mei, N. L. Leung, R. T. Kwok, J. W. Lam and B. Z. Tang, *Chem. Rev*., 2015, **115**, 11718-11940.

31 W. P. Jencks, *Prog. Phys. Org. Chem*., 1964, **2**, 63-128.

32 V. Novakova, P. Zimcik, M. Miletin, L. Vachova, K. Kopecky, K. Lang, P. Chábera and T. Polívka, *Phys. Chem. Chem. Phys.*, 2010, **12**, 2555-2563.

33 Gaussian 09, Revision A.02, M. J. Frisch, G. W. Trucks, H. B. Schlegel, G. E. Scuseria, M. A. Robb, J. R. Cheeseman, G. Scalmani, V. Barone, G. A. Petersson, H. Nakatsuji, X. Li, M. Caricato, A. Marenich, J. Bloino, B. G. Janesko, R. Gomperts, B. Mennucci, H. P. Hratchian, J. V. Ortiz, A. F. Izmaylov, J. L. Sonnenberg, D. Williams-Young, F. Ding, F. Lipparini, F. Egidi, J. Goings, B. Peng, A. Petrone, T. Henderson, D. Ranasinghe, V. G. Zakrzewski, J. Gao, N. Rega, G. Zheng, W. Liang, M. Hada, M. Ehara, K. Toyota, R. Fukuda, J. Hasegawa, M. Ishida, T. Nakajima, Y. Honda, O. Kitao, H. Nakai, T. Vreven, K. Throssell, J. A. Montgomery, Jr., J. E. Peralta, F. Ogliaro, M. Bearpark, J. J. Heyd, E. Brothers, K. N. Kudin, V. N. Staroverov, T. Keith, R. Kobayashi, J. Normand, K. Raghavachari, A. Rendell, J. C. Burant, S. S. Iyengar, J. Tomasi, M. Cossi, J. M. Millam, M. Klene, C. Adamo, R. Cammi, J. W. Ochterski, R. L. Martin, K. Morokuma, O. Farkas, J. B. Foresman, and D. J. Fox, Gaussian, Inc., Wallingford CT, 2016.